Biofilm re-vitalization using hydrodynamic shear stress for stable power generation in microbial fuel cell

ISLAM, M Amirul, EHIRAJ, Baranitharan, CHENG, Chin Kui, DUBEY, Bipro <http://orcid.org/0000-0003-0396-9864> and KHAN, Md Maksudur Rahman

Biofilm re-vitalization using hydrodynamic shear stress for stable power generation in microbial fuel cell

M. Amirul Islam, Baranitharan Ehiraj, Chin Kui Cheng, Bipro Nath Dubey, Md Maksudur Rahman Khan

PII: S1572-6657(19)30363-7
DOI: https://doi.org/10.1016/j.jelechem.2019.05.013
Reference: JEAC 13131

To appear in: *Journal of Electroanalytical Chemistry*

Received date: 4 April 2018
Revised date: 19 March 2019
Accepted date: 6 May 2019

Please cite this article as: M.A. Islam, B. Ehiraj, C.K. Cheng, et al., Biofilm re-vitalization using hydrodynamic shear stress for stable power generation in microbial fuel cell, Journal of Electroanalytical Chemistry, https://doi.org/10.1016/j.jelechem.2019.05.013

Biofilm re-vitalization using hydrodynamic shear stress for stable power generation in microbial fuel cell

M Amirul Islam[a,d], Baranitharan Ehiraj[a,e], Chin Kui Cheng[a,b], Bipro Nath Dubey[c], Md Maksudur Rahman Khan[a,b]*

[a]Faculty of Chemical and Natural Resources Engineering, Universiti Malaysia Pahang, 26300 Gambang Pahang, Malaysia.

[b]Centre of Excellence for Advanced Research in Fluid Flow (CARIFF), Universiti Malaysia Pahang, 26300 Gambang Pahang, Malaysia.

[c]Faculty of Arts, Computing, Engineering and Sciences, Sheffield Hallam University, Howard Street, Sheffield, UK

[d]Interdisciplinary Institute for Technological Innovation (3IT), Laboratory for Quantum Semiconductors and Photon-based BioNanotechnology, Université de Sherbrooke, 3000, boul. de l'Université, Sherbrooke, Québec J1K 0A5, Canada

[e]Department of Biotechnology, Saveetha School of Engineering, Saveetha University, Chennai, Tamil Nadu, India

* To whom correspondence should be addressed.

E-mail: mrkhancep@yahoo.com, mrkhan@ump.edu.my

Tel.: +609-5492872

Abstract

Viable electroactive biofilm formation, allowing considerable conversion capacity and opportunities for extracellular electron transfer (EET) is essential for sustainable and long term stable power generation in microbial fuel cells (MFCs). However, over the time, the anodic biofilm can be particularly detrimental for electrogenesis due to the accumulation of more dead cells and that increases the charge transfer resistance as well as reduces the electrocatalytic efficiency. In this study, flow induced shear stresses (4.38, 9.34 and 14.92 mPa) were employed to revitalize the biofilm by removing the inert biomass for the maintenance of stable power in MFCs. Among them, the moderate shear stress (9.34 mPa) successfully reduced the thickness and thereby revitalized the biofilm within a short time. The field emission scanning electron microscopy (FESEM) and cell viability count analysis of the biofilms confirmed that the shear stress (9.34 mPa) reduced the dead cells accumulation in the biofilm. Moreover, this treatment significantly reduced the polarization resistance (68%) by dislodging nonconductive inert dead cells from the surface. Our results revealed that the application of shear stress could be an effective method to maintain the stable power generation by reducing the thickness and increasing the cell viability of the biofilm in the MFC.

Key words: Electroactive biofilm; *Pseudomonas aeruginosa*; Resistance; Shear stress; Palm oil mill effluent

1. Introduction

Electro-active biofilm with higher electron discharging capacity is a key factor for developing strategies to optimize the power generation of microbial fuel cells (MFCs) [1]. In recent studies [2, 3], it has been reported that the variable biocatalyst density associated with microbial growth and its decay is a unique feature of MFC which mainly affects its power generation. Excessive bacterial colonization on the anode over time brings high resistance to the substrate diffusion as well as to the charge transfer [4, 5]. Some recent studies reported that the metabolic status of biofilms such as conductivity, rates of diffusion of substrates and end products can affect the bacterial growth in thick electrogenic biofilms [3, 6, 7]. The analysis on the structures of the biofilms over time demonstrated the formation of a live outer-layer that covers the dead inner-core of the biofilm [6, 8]. This double layer structure appeared because, during biofilm development, the live layer reached a constant thickness, whereas dead cells continued to accumulate near to the electrode surface due to the lack of nutrients which merely functioned as an electrically conductive matrix and was responsible for low current generation [3, 9].

The stable power generation is an important requirement to exploit MFC in practical applications [10]. Our recent study [11] showed that the MFC could achieve stable power generation until certain days of operation; however, over time, the dead cells start accumulating on the anode surface which substantially reduced the performance of MFC. The detrimental effects of thick biofilm on MFC performance can be alleviated by retrenching the thickness of biofilm as well as through the removal of excess inert biomass [11, 12]. Therefore, in order to avoid the formation of dead core biofilm, several techniques can be used for biofilm cleaning which can maintain the biofilm thin so that the accumulation of more dead cells can be avoided. Up to now, only a few attempts have been made to solve this issue but truly effective and

practical countermeasures are still lacking. So far, several methods such as oxygenation, flow rate, rotation, chemical (antibiotic), enzymatic treatment, mechanical cleaning etc. have been implemented to remove inert biomass (dead cells) from the surface [13-15]. However, these systems cannot be considered as sustainable and feasible method due to their toxicity, conflicting environmental issues and inapplicability in large scale systems [14, 16]. Therefore, cleaning the water distribution system via flushing (shear stress) flow, pigging is considered to be the best methods for large scale biofilm control [17].

Recently, several methods such as chemical and mechanical assisted biofilm deformation have been employed for the removal of biofilm in different bioreactor systems especially in membrane bioreactor (MBR) [18]. However, none of these studies were conducted to clean the electrode surface in the bio-electrochemical (BES) cells. It is important to note that the performance of MBR deteriorates due to the formation of biofilm[19]. But, unlike MBR system, MFC requires biofilm to generate electricity [20]. Therefore, the revitalization of biofilm is emergent instead of total biofilm removal in MFC system.

In this context, a shear stress induced biofilm revitalization technique has been developed and the efficiency of this method has been evaluated. Furthermore, the status of biofilm was analyzed by FESEM, EIS, CV and cell viability count and was correlated with power generation of MFC.

2. Experimental Methods

2.1 Sample collection and characterization

The palm oil mill effluent (POME) was collected from LKPP Corporation Sdn. Bhd., Gambang, Pahang and stored at 4 °C to prevent the deterioration of ingredients. The solids and debris were removed through a Whatman No.1 filter paper and subsequently, the wastewater was sterilized

by autoclaving at 121 °C for 15 min before it was used as the culture medium. All the experiments were conducted using POME as the substrate without adding additional nutrients.

2.2 Isolation and characterization of bacteria

The pure culture bacterium (*P. aeruginosa*) was isolated from the municipal wastewater (drainage discharge point) of Kuantan, Pahang, Malaysia. The pure cultures were enriched by preparing an overnight culture in Luria Bertani broth (10% v/v) and incubated at 35°C in a shaker incubator (150 rpm). The 1 mL of broth culture was used as inoculum in the MFC. The molecular analysis and phylogenetic relationship of bacteria have been described by Islam et al. [21]

2.3 MFC assembly and operation

The MFC experiments were operated at room temperature (27 ± 2 °C) in batch mode. Six dual chamber MFCs (MFC_1-MFC_6) were fabricated using a cubic plexi glass (10 cm x 10 cm x 10 cm) with the working volume of 20 mL (Shanghai, Sunny Scientific, China). Carbon felt (5 x 0.8 x 5 cm) was used as anode and cathode electrodes in all the experiments. The electrodes were cleaned with 1.0 M NaOH and subsequently with 0.1 M H_2SO_4 after each experiment and stored in distilled water before use. A cation exchange membrane (Nafion 117, Dupont Co., USA) was used to separate the anode and cathode compartments of MFC. Prior to use, the Nafion membrane was pre-treated using dilute HCl for 1 hour and subsequently boiled in Deionized (DI) water for about 1 h. After the whole MFC set up was tighten up with screws, the anode compartment was filled with sterilized 50% POME (20 mL) and subsequently, the pure culture bacteria (1 mL) were inoculated into it while the cathode chamber was filled with $KMnO_4$ solution, as an oxidizing agent. The anode and cathode electrodes were connected by using

titanium wires with a rheostat (Crotech DRB-9, UK) to form a circuit. The whole set-up was connected with peristaltic pump and shear stress (4.39 mPa, 9.34 mPa and 14.92 mPa) was employed for about 5 minutes when needed. The whole set-up was connected with peristaltic pump and flow induced shear stress was employed for about 5 minutes by applying the flush flowrates of 500 mL/min (4.39 mPa), 1000 mL/min (9.34 mPa) and 1500 mL/min (14.92 mPa) for 5 min when needed. The schematic diagram of experimental set-up has been presented in Fig. S1.

2.4 Cell viability count of biofilm

The fluorescence microscope (Olympus BX53, Germany) with 20X objective lens was employed to determine the cell viability with the help of LIVE/DEAD Bacterial Viability Kit (BD™ Cell Viability Kit). In brief, cell viability of biofilm was performed by detruncating small part (1 cm) of the anode using a sterilized scissor and then immediately immersed in the 50 mM phosphate buffer. In order to separate the microorganisms from carbon brush, it was centrifuged for about 1 min (5000 rpm), thereafter; cell suspension was serially diluted and stained using a viability staining kit. Finally, stained cells were filtered through 0.4 µm membrane filter and counted using a microscope. The cell density per anode geometric area was determined using the dilution factor, the filtered volume and the ratio of total filtered area to image area [2]. The method was replicated using 4-6-diamidino-2-phenyl indole (DAPI) for comparison. All experiments were replicated for three times.

2.5 FESEM analysis of the biofilm

Biofilm formation on the anode electrode was visualized using FESEM (5 kV) at various time intervals of the MFC experiments. The small sections of the anodes were cut off from the anode

compartment and rinsed using sterile water. Subsequently, it was soaked in a beaker containing anaerobic solution of glutaraldehyde (3%). The samples were then washed twice with 0.1 M phosphate buffer and dehydrated successively at various ethanol concentrations for about 10 minutes. After that, the samples were dried and coated with platinum to a thickness of 10 nm. Finally, the specimens were observed by FESEM. All experiments were replicated for three times.

2.6 Analyses and calculations

Polarization measurements were performed at regular intervals (15 min) to estimate the power production of MFC at various external resistances ranging from 50 to 20,000Ω using an external resistor. The voltage data were taken using a digital multimeter with built in data logger (Fluke 289 true RMS industrial logging digital multimeter, USA) after it reached the stable value for obtaining the polarization curves. Power density normalized by volume (P_V, W/m^3) was calculated using the following equation.

$$P_v = U^2/vR \quad (1)$$

where P is the power (Watt), U is the voltage, v is the volume and R is the resistance.

At laminar condition, the average shear rate ($\dot{\gamma}$) and shear stress (τ) in a pipe flow can be estimated as following

$$\dot{\gamma} = 8u/d \text{ and } \tau = \mu\dot{\gamma} \quad (2)$$

where d is the diameter of the cylindrical cell; u is the average velocity of the fluid through the cell and μ is the liquid average viscosity (Newtonian).

The COD removal efficiency and columbic efficiency of dual chamber MFC was calculated as

described by Baranitharan et al. [22]. The COD was determined using a COD reactor (HACH DRB 200, USA). The COD removal efficiency was calculated using equation (2)

$$COD\ removal\ efficiency = \frac{COD_i - COD_t}{COD_t} \times 100 \quad (3)$$

where, COD_i and COD_t represent the initial COD (mg/L) of the anode chamber and the COD of the anode chamber at a particular time. All experiments were replicated for three times.

2.7 Electrochemical analysis

2.7.1 Cyclic voltammetry analysis

Cyclic voltammetry (CV) was used to examine the catalytic behaviour of the MFCs. The CV analysis aids in characterizing the electron transfer interactions between the biofilm (biocatalyst) and the anode electrode of the MFC. Moreover, it helps to reveal the precise role of redox mediators, cytochromes and pili in the electrochemical reactions [23]. The CV was performed using an electrochemical system, PARSTAT 2273, USA. A three electrode system was applied to collect the CV data where anode and cathode were used as working and counter electrodes respectively. The Silver/Silver chloride (1.0 M KCl) electrode was disinfected using 70% ethanol (Sigma) and used as a reference electrode. Moreover, the reference electrode was placed closer to the anode surface during CV operation. The CV was performed at a scan rate of 30 mV/s within the potential range of +1.0 to -1.0 V and before each measurement; nitrogen gas was purged for about 15 min.

2.7.2 Electrochemical impedance spectroscopy

Electrochemical impedance spectroscopy (EIS) measurements were performed using a potentiostat, PARSTAT 2273, USA. In order to analyze the anodic internal resistances of MFC, a three electrode system was used where the anode and cathode electrode was used as working and counter electrode, respectively. The Silver/Silver chloride electrode (1.0 M KCl) was used as the reference electrode. An AC signal (10 mV, 100 kHz – 5 mHz) was applied to prevent the biofilm detachment as well as to minimize the disturbance on systematic stability. The EIS data were fitted with the equivalent circuit (EC): [R(RQ)(R[QT])] using Nova 1.11 software.

3. Results and discussion

3.1. Performance of MFC in batch mode

The MFC (MFC_1) was operated for 25 days in batch mode using POME (COD = 23,258 mg/L) as substrate. The performance of MFC was recorded every 2 days as shown in Fig. 1a and 1b. It can be seen that the power generation gradually increased and achieved the power density of 2.7 W/m^3 on 1^{st} day (after 18 hours) of operation and thereafter it sharply increased until 6 days of operation. After that, it maintained the stable value until the 17^{th} day where the maximum performance of 6.1 W/m^3 was achieved on the 11^{th} day, and then the power generation sharply decreased and reached to 3.6 W/m^3 on the 25^{th} day. It is important to note that the performance was sharply dropped even though the COD content was higher (10,222 mg/L) in the anode compartment after 20 days of operation.

The CV and Nyquist plots for the anode configuration on day 3, 11 and 21 have been presented in Fig. 1c and 1d. It can be seen that, on the 3^{rd} day, less intense redox peak (Fig. 1c), higher anode R_{ct} (287.33 Ω, Fig. 1d) and lower diffusion resistance (28.46 Ω, Table S1) were obtained which might be due to the presence of fewer microbes as well as less electron shuttle

compounds in the MFC_1. However, on the 11th day, intense redox peak (increased by 60%), lower anode R_{ct} (reduced by 82%) and moderate diffusion resistance (58.89 Ω, Table S1) were obtained, presumably due to an increase in biocatalyst density in both bulk as well as in the biofilm thereby enhanced the amount of endogenously produced compounds that may aid in extracellular electron transfer [2, 24]. While on 21st day, the anode R_{ct} and diffusion resistance were again increased and reached to 178.56 Ω and 191.43 Ω respectively, resulting in a significant reduction in redox activity. It is important to note that the intense reversible redox peak which was obtained in MFC_1 but was not detected in the control cell (MFC without inoculation) suggesting that the electrochemical activity was mainly because of the redox mediators excreted by the microorganisms [25, 26]. Previous studies reported that, *P. aeruginosa* could produce phenazines as soluble redox mediators and that facilitates the extracellular electron transfer between bacterial cells and electrode [27, 28] in MFCs.

The drastic reduction in power generation after 17 days of operation might be due to the factors, such as electrode fouling, membrane blockage, catalyst inactivation, substrate depletion and excessive growth of biofilms etc. [29, 30]. To observe the effect of biofilm thickness on MFC performance, the biofilm was visualized using FESEM on different days of operation as presented in Fig. 1e - 1g. On the 3rd day, only a few microorganisms were observed around the electrode surface as shown in Fig. 1e. Thereafter, the microorganisms formed colonies and embedded in a self-produced extracellular matrix of polymeric substances produced by them. Thus, the effective biofilm formation was achieved on the 11th day of operation (Fig. 1f). However, on the 21st day, multilayer thick biofilm was formed (Fig. 1g) which would have decreased the power generation of MFCs. In general, *P. aeruginosa* is capable to develop thick biofilm within a short period of time which could be an average size of 33 microns [31]. Sun et

al. [30] observed the highest electrochemical activity when the thickness of biofilm reached to ~20 mm and found that the electrochemical activity decreased with increasing thickness of biofilm. In addition, bacterial cell viability of the biofilm was also analyzed on different days of MFC_1 operation and presented in Fig. 1h. The number of live cells increased with the time until 11^{th} day of operation where live cells outnumbered the dead cells. However, it should also be noted that the number of dead cells increasing from day 3, and eventually exceeded the number of live cells by many folds on the 21^{st} day which might be due to the hindrance in diffusion of substrates from outer-layer of the biofilm to the inner layer.

3.2 Effect of biofilm removal on power generation

3.2.1 Mechanical removal

In order to observe the effect of biofilm removal on MFC performance, another cell (MFC_2) was operated similar to MFC_1 (Fig. 1a) but, in MFC_2, after 21 days of operation, the carbon felt was taken out from the anode chamber, and the biofilm from the surface of the felt was completely removed using the sterile brush in laminar air condition, and finally, it was autoclaved for 2 hours. Thereafter, the felt was placed again in the anode compartment and continued to run in the MFC_2. The current generation went up sharply and on 25^{th} day, it reached the stable value. In MFC_2, the biofilm formation was analyzed using FESEM and the images of the anode (before and after removal) are presented in Fig. 2b and 2c. In Fig. 2b, after 21^{st} day, very thick layer of biofilm was observed whereas, after the removal of biofilm on 22^{nd} day, very less microbes were found around the electrode surface as shown in Fig. 2c. Bacterial cell viability of the biofilm was analyzed on different days of MFC_2 operation and presented in Fig. 2d. On 21^{st} day, the number of dead cells increased significantly and outnumbered the live cells by 4.5 fold. However, on 25^{th}

day, very less number of dead cells were observed due to the immediate removal of thick biofilm (On 22nd day) comprising with inert biomass (dead cells). In general, bacteria can form thin biofilm within few days of MFC operation and the cells then increase continuously and forms an ineffective multilayer biofilm comprising with outnumber of dead cells [3, 32] that could deteriorate the power generation of MFC.

In Fig. 2e, the CV peak was observed at 0.054 A on 21st day, however, the catalytic efficiency increased and reached to 0.12 A on 25th day. The enhancement in catalytic efficiency on the 25th day of operation clearly indicates the occurrence of biofilm reformation. Moreover, the polarization resistance was observed as 238.56 Ω on day 21 (Fig. 2f), indicating the accumulation of more dead cells on the surface of the anode (Fig. 2d). But, after the removal of ineffective thick biofilm and subsequent operation, the polarization resistance was reduced to 78.32 Ω (25th day). These results revealed that after certain days of operation the anode biofilm become ineffective due to the reduced metabolic activity of the biofilm and the revitalization of biofilm can positively influences the electrochemical transport processes and restores the MFC performance. Moreover, it showed that live-cell mass are needed rather than thick biofilm to obtain higher metabolic activity as well as higher current generation. Our previous study [33] also showed that the redox peak significantly reduced due to the formation of multilayer biofilm comprising more dead cells, and this dead inner layer hindered the electron transfer from the live bacteria present in the outer layer of the biofilm and bulk solution. Besides that, the electrons in the biofilm needed to travel over substantial distances to reach the anode and the resistance associated with long distance electron transport is substantially higher than the resistance associated with the single electron transfer step from the biofilm to the anode at the biofilm/anode interface [34]. In our previous studies [10, 21], we also observed that the *P.*

aeruginosa transferred electron through the electron shuttling mechanism. Hence, the electron transfer through the biofilm which either uses direct or mediated electron transfer or both might be hindered by the dead cells and the inert biomass of the biofilm on the anode electrode surface [3].

3.2.2 Flow induced removal

To observe the effect of shear stress on ineffective thick biofilm and its influence on MFC performance, three MFCs (MFC_3-MFC_5) were operated under similar conditions but when the current generation was dropped (after 21 days), different shear stresses (4.38, 9.34 and 14.92 mPa) were applied to different MFCs (MFC_3-MFC_5) for about 5 min as shown in Fig. 3a - 3c. It was observed that the current generation dropped after 21 days and did not fully recover even though the flow induced shear stress of 4.38 mPa was applied. On the other hand, when the shear stress was doubled (9.34 mPa), the current generation increased and did not drop until the end of the operation. However, while the shear stress was high (14.92 mPa), the current generation was slowly increased and also not able to reach to the maximum. The effect of shear stress on performance was also further confirmed by polarization data. The polarization data was recorded on 25^{th} day for different shear stress as presented in Fig. 3d. It can be observed that among the three different shear stresses, the moderate shear stress (9.34 mPa) achieved a maximum power density of 5.8 W/m^3 whereas low (4.38 mPa) and high shear stress (14.32 mPa) achieved 3.5 W/m^3 and 2.8 W/m^3 respectively.

The anode biofilm was visualized (on 22^{nd} day) under FESEM to observe the effect of shear stress, as shown in Fig. 4. At low shear stress (4.38 mPa), a very small number of cells were removed from the electrode surface (Fig. 4b). But, after applying the moderate shear stress (9.34 mPa), most of the cell colonies were removed but still, some number of microorganisms

were observed around the electrode surface (Fig. 4c). While high shear stress (14.92 mPa) was applied, very few microorganisms were observed around the electrode surface indicating the complete detachment of biofilm from the surface. The variation in the thickness of biofilm for different shear stresses can help to explain why the performance of MFCs varied for different shear stresses. At strong shear stress (14.92), most of the cells from the electrode surface were removed (Fig. 3d) causing long time to reestablish the biofilm. Thus, it could not achieve stable power generation since it will take long time to form the effective biofilm. However, in case of moderate shear stress (9.34 mPa), most of the ineffective biofilm as well as cellular waste products were removed from the electrode surface and therefore the current generation reached to the maximum and not dropped immediately (Fig. 3b) [35]. On the other hand, under the low shear stress (4.38 mPa), the current generation could not be able to achieve the maximum value and also dropped immediately, might be due to the incomplete detachment of inert biomass on the anode surface (Fig. 3b).

EIS and CV were measured on 25th day (while the current generation reached the stable value), as shown in Fig. 5a and 5b. It can be seen that, the low shear stress (4.38 mPa) achieved higher R_{ct} (98.76 Ω) and small redox peak (maximum current 0.017 A) suggesting that the multilayer biofilm immediately formed on anode surface due to the incomplete removal of inactive biomass [36]. Among the shear stresses, the moderate shear stress (9.34 mPa) achieved lower R_{ct} (68.52 Ω) and strong redox peak (0.024 A) indicating the salient electrochemical activities of bacteria and the presence of more redox active compounds in the anode biofilm [11, 37]. The higher electrochemical activity ascribe that the higher number of active cells in the biofilm and bulk [33, 38]. Furthermore, it promotes the formation of thin biofilm which allows the nutrients to pass through easily into the biofilm thereby achieved higher active biomass

within a short period of time [39]. But, in case of high shear stress application, the MFC showed higher R_{ct} (237.32 Ω) and poor bioelectrocatalytic activity (0.0097 A) which might be due to the absence of effective biofilm on the electrode surface. The anode diffusion resistances for low, moderate and high shear stresses were found to be 118.98 Ω, 92.67 Ω and 101.23 Ω respectively. The moderate shear stress obtained lower diffusion resistance compared to others (Table S1) indicating the formation of conductive/efficient biofilm with shorter diffusion path. Efficient biofilm meant the the biofilm consisting of significant number of active cells on the surface of anode electrode. The presence of thin biofilm with higher active cells at the vicinity of the electrode consequently reduced the diffusion path resulting in a lower diffusion resistance in co-culture inoculated MFC. In contrast, higher diffusion resistance was observed for other shear stresses which might be due to the presence of less efficient biofilm on the surface of the electrode [21]. Additionally, the use of moderate shear stress obtained higher capacitance (11.18 µF) compared to other shear stresses (Table S1) indicating that it can achieve higher bio-capacitance and lower $R_{ct,}$ thereby enhancing the performance of MFC.

In this study, under a shear stress of 4.38 mPa, the current generation slightly increased and then dropped immediately, which might be due to the incomplete detachment of inert biomass on the anode surface (Fig. 4b). Besides that, specific EPS components, such as the Psl exo-polysaccharides formed by *P. aeruginosa* biofilms have been known to increase the elasticity and cross-linking within the matrix is thought to facilitate the formation of micro-colonies [40]. Thus the chances of forming thick biofilm again are more and can negatively influence the power generation of MFCs. Rochex and Lebeault [41] reported that in biofilm formation process, lower hydrodynamic conditions strongly influences transport rates of oxygen, nutrients and cells from the fluid to the biofilm, the effect of flow conditions on the structural

plasticity of biofilms (mass transfer limitations) and the cellular induced reactions, acting as single or concomitant factors. While moderate shear stress (9.34 mPa) was applied both the ineffective thick biofilm as well as the cellular waste products were removed and therefore the current generation reached to the maximum and not dropped until the end of the operation [35]. Moreover, the cell growth rate might be increased due to moderate shear stress, which consecutively enhanced the power generation in MFC [16]. Manuel et al. [42] reported that in fixed biofilm systems, the moderate shear stress have the advantage of limiting biofilm growth since they produce thinner layers and therefore the biofilm can be revitalized with more live cells. In another study, Liu et al. [16] reported that the nutrient transport rate from bulk water into the biofilm increases at moderate shear stress and, that in turn, stimulates further cell growth in biofilms. Therefore, it is clear that moderate shear stress (9.34 mPa) can stimulate the formation of effective biofilm within a short period of time. But, in case of high shear stress (14.92 mPa), the current generation increased very slowly which might be due to the complete removal of metabolic cells from the anode biofilm (Fig. 4d). Besides that, when high external shearing forces imposed to the biofilm the internal cohesive strength of biofilm matrix exceed; thereby, the biofilm detachment can be achieved either by the increase in the external forces or by the decrease in the internal forces [43, 44]. Furthermore, at high shear stress, most of the cells from the electrode surface were removed causing a long time to re-establish the biofilm. Thus, it could not achieve stable power generation since it would take a long time to form the effective biofilm.

Our study showed that the performance of MFC started to drop sharply after 18 days of operation when the number of dead cells exceeded the live cells on anode surface (Fig. 1h). The deterioration of MFC performance can be prevented or minimized using moderate shear stress

(9.34 mPa), which dislodges particles such as inert biomass and nonconductive debris from the surface of the anode. Therefore, in order to achieve an uninterrupted stable MFC performance another MFC (MFC_6) was operated and applied shear stress (9.34 mPa) after 18 days of operation and thereafter, for every 6 days of interval the same technique was applied (Fig. S2). It is important to note from the Fig. 1f that the complete aging of biofilm occurs within 10 days of operation. The intervention in that process is required within that time interval. Therefore, the flow shear stress was applied at an interval of 6 days. It can be seen that the current generation was not dropped and maintained the stable performance until 40^{th} day of operation.

4. Conclusions

MFCs, especially operated with real wastewaters, inevitably suffer from performance deterioration with severe fluctuations in the power generation. The formation of thick biofilm is one of the major internal deteriorations responsible for the decline in MFC performance. Therefore, improving the availability of effective microorganisms within the biofilm becomes crucial for reducing the fluctuations during power generation in MFCs. In this study, we have successfully used flow induced shear stress technique to revitalize the biofilm for maintaining the stable power generation in MFC. The FESEM, CV and EIS results revealed that the formation of multilayer thick biofilm comprising with outnumber of dead cells increased the charge transfer resistance and thereby reduced the electrocatalytic efficiency. In order to revitalize the biofilm, different shear stresses were applied. Among the shear stresses used, the moderate shear stress (9.34 mPa) has effectively removed the dead cells/inert debris and revitalized the biofilm with effective microorganisms in a short time. The results suggest that this technique can potentially be applied for long term stable power generation in MFCs.

Author Information

Corresponding Author

*E-mail: mrkhancep@yahoo.com, mrkhan@ump.edu.my. Tel: +6095492872.

ORCID: Md. Maksudur Rahman Khan: 0000-0001-6594-5361

Present Address

Faculty of Chemical and Natural Resources Engineering, Universiti Malaysia Pahang, 26300 Kuantan, Malaysia.

Notes

The authors declare no competing financial interest.

Acknowledgements

This work was supported by the University Malaysia Pahang, Malaysia (RDU 140322 and GRS 150371) and Newton Research Collaboration Programme (NRCP1617/5/42).

References

[1] S.T. Read, P. Dutta, P.L. Bond, J. Keller, K. Rabaey, Initial development and structure of biofilms on microbial fuel cell anodes, BMC Microbiol. 10(1) (2010) 98.

[2] Z. Ren, R.P. Ramasamy, S.R. Cloud-Owen, H. Yan, M.M. Mench, J.M. Regan, Time-course correlation of biofilm properties and electrochemical performance in single-chamber microbial fuel cells, Bioresour. Technol. 102(1) (2011) 416-421.

[3] D. Sun, S. Cheng, A. Wang, F. Li, B.E. Logan, K. Cen, Temporal-Spatial Changes in Viabilities and Electrochemical Properties of Anode Biofilms, Environ. Sci. Technol. 49(8) (2015) 5227-5235.

[4] I. Ieropoulos, J. Winfield, J. Greenman, Effects of flow-rate, inoculum and time on the internal resistance of microbial fuel cells, Bioresour. Technol. 101(10) (2010) 3520-3525.

[5] S.A. Patil, F. Harnisch, B. Kapadnis, U. Schröder, Electroactive mixed culture biofilms in microbial bioelectrochemical systems: the role of temperature for biofilm formation and performance, Biosens. Bioelectron. 26(2) (2010) 803-808.

[6] E.G. Di Domenico, G. Petroni, D. Mancini, A. Geri, L.D. Palma, F. Ascenzioni, Development of Electroactive and Anaerobic Ammonium-Oxidizing (Anammox) Biofilms from Digestate in Microbial Fuel Cells, BioMed research international (2015).

[7] D. Sun, A. Wang, S. Cheng, M. Yates, B.E. Logan, *Geobacter anodireducens* sp. nov., an exoelectrogenic microbe in bioelectrochemical systems, Int. J. Syst. Evol. Microbiol. 64(10) (2014) 3485-3491.

[8] S. Chen, X. Jing, J. Tang, Y. Fang, S. Zhou, Quorum Sensing Signals Enhance the Electrochemical Activity and Energy Recovery of Mixed-Culture Electroactive Biofilms, Biosens. Bioelectron. (2017).

[9] Y. Yang, D. Ye, Q. Liao, P. Zhang, X. Zhu, J. Li, Q. Fu, Enhanced biofilm distribution and cell performance of microfluidic microbial fuel cells with multiple anolyte inlets, Biosens. Bioelectron. 79 (2016) 406-410.

[10] M.A. Islam, H.R. Ong, B. Ethiraj, C.K. Cheng, M.M.R. Khan, Optimization of co-culture inoculated microbial fuel cell performance using response surface methodology, Journal of environmental management 225 (2018) 242-251.

[11] M.A. Islam, C.W. Woon, B. Ethiraj, C.K. Cheng, A. Yousuf, M.M.R. Khan, Ultrasound driven biofilm removal for stable power generation in microbial fuel cell, Energy Fuels 31(1) (2016) 968-976.

[12] A. Kato Marcus, C.I. Torres, B.E. Rittmann, Conduction- based modeling of the biofilm anode of a microbial fuel cell, Biotechnol. Bioeng. 98(6) (2007) 1171-1182.

[13] L. Janczewski, A. Trusek-Holownia, Biofilm-based membrane reactors–selected aspects of the application and microbial layer control, Desalination and Water Treatment (2015) 1-8.

[14] T. Nguyen, F.A. Roddick, L. Fan, Biofouling of water treatment membranes: a review of the underlying causes, monitoring techniques and control measures, Membranes 2(4) (2012) 804-840.

[15] M.A. Islam, C.W. Woon, B. Ethiraj, C.K. Cheng, A. Yousuf, M.M.R. Khan, Correlation of power generation with time-course biofilm architecture using *Klebsiella variicola* in dual chamber microbial fuel cell, Int. J. Hydrogen Energy 42(41) (2017) 25933-25941.

[16] S. Liu, C. Gunawan, N. Barraud, S.A. Rice, E.J. Harry, R. Amal, Understanding, Monitoring, and Controlling Biofilm Growth in Drinking Water Distribution Systems, Work 5 (2016) 7.

[17] M.J. Lehtola, T.K. Nissinen, I.T. Miettinen, P.J. Martikainen, T. Vartiainen, Removal of soft deposits from the distribution system improves the drinking water quality, Water Res. 38(3) (2004) 601-610.

[18] E.R. Brindle, D.A. Miller, P.S. Stewart, Hydrodynamic deformation and removal of *Staphylococcus epidermidis* biofilms treated with urea, chlorhexidine, iron chloride, or DispersinB, Biotechnol. Bioeng. 108(12) (2011) 2968-2977.

[19] C. Williams, R. Wakeman, Membrane fouling and alternative techniques for its alleviation, Membrane technology 2000(124) (2000) 4-10.

[20] O. Ichihashi, T.A. Vishnivetskaya, A.P. Borole, High- Performance Bioanode Development for Fermentable Substrates via Controlled Electroactive Biofilm Growth, ChemElectroChem 1(11) (2014) 1940-1947.

[21] M.A. Islam, B. Ethiraj, C.K. Cheng, A. Yousuf, M.M.R. Khan, An Insight of Synergy between *Pseudomonas aeruginosa* and *Klebsiella variicola* in a Microbial Fuel Cell, ACS Sustainable Chemistry & Engineering 6(3) (2018) 4130-4137.

[22] E. Baranitharan, M.R. Khan, D. Prasad, J.B. Salihon, Bioelectricity generation from palm oil mill effluent in microbial fuel cell using polacrylonitrile carbon felt as electrode, Water, Air, Soil Pollut. 224(5) (2013) 1-11.

[23] J.L. Varanasi, A.K. Nayak, Y. Sohn, D. Pradhan, D. Das, Improvement of power generation of microbial fuel cell by integrating tungsten oxide electrocatalyst with pure or mixed culture biocatalysts, Electrochim. Acta 199 (2016) 154-163.

[24] M. Rahimnejad, A.A. Ghoreyshi, G. Najafpour, T. Jafary, Power generation from organic substrate in batch and continuous flow microbial fuel cell operations, Applied Energy 88(11) (2011) 3999-4004.

[25] M.A. Islam, B. Ethiraj, C.K. Cheng, A. Yousuf, M.M.R. Khan, Electrogenic and Antimethanogenic Properties of *Bacillus cereus* for Enhanced Power Generation in Anaerobic Sludge-Driven Microbial Fuel Cells, Energy Fuels 31(6) (2017) 6132-6139.

[26] Y. Asensio, C. Fernandez-Marchante, J. Lobato, P. Cañizares, M. Rodrigo, Influence of the ion-exchange membrane on the performance of double-compartment microbial fuel cells, J. Electroanal. Chem. 808 (2018) 427-432.

[27] V.B. Wang, S.-L. Chua, B. Cao, T. Seviour, V.J. Nesatyy, E. Marsili, S. Kjelleberg, M. Givskov, T. Tolker-Nielsen, H. Song, Engineering PQS biosynthesis pathway for enhancement of bioelectricity production in *Pseudomonas aeruginosa* microbial fuel cells, PLoS One 8(5) (2013) e63129.

[28] Y. Qiao, Y.-J. Qiao, L. Zou, C.-X. Ma, J.-H. Liu, Real-time monitoring of phenazines excretion in *Pseudomonas aeruginosa* microbial fuel cell anode using cavity microelectrodes, Bioresour. Technol. 198 (2015) 1-6.

[29] M. Sun, L.-F. Zhai, W.-W. Li, H.-Q. Yu, Harvest and utilization of chemical energy in wastes by microbial fuel cells, Chem. Soc. Rev. 45(10) (2016) 2847-2870.

[30] D. Sun, J. Chen, H. Huang, W. Liu, Y. Ye, S. Cheng, The effect of biofilm thickness on electrochemical activity of Geobacter sulfurreducens, Int. J. Hydrogen Energy 41(37) (2016) 16523-16528.

[31] B.M. Peyton, Effects of shear stress and substrate loading rate on *Pseudomonas aeruginosa* biofilm thickness and density, Water Res. 30(1) (1996) 29-36.

[32] M. Moradi, Z. Song, X. Nie, M. Yan, F.Q. Hu, Investigation of bacterial attachment and biofilm formation of two different *Pseudoalteromonas* species: Comparison of different methods, Int. J. Adhes. Adhes. 65 (2016) 70-78.

[33] M.A. Islam, B. Ethiraj, C.K. Cheng, A. Yousuf, S. Thiruvenkadam, R. Prasad, M.M. Rahman Khan, Enhanced Current Generation Using Mutualistic Interaction of Yeast-Bacterial Coculture in Dual Chamber Microbial Fuel Cell, Ind. Eng. Chem. Res. 57(3) (2018) 813-821.

[34] N.S. Malvankar, M.T. Tuominen, D.R. Lovley, Biofilm conductivity is a decisive variable for high-current-density Geobacter sulfurreducens microbial fuel cells, Energy Environ. Sci. 5(2) (2012) 5790-5797.

[35] W.G. Pitt, S.A. Ross, Ultrasound increases the rate of bacterial cell growth, Biotechnol. Prog. 19(3) (2003) 1038-1044.

[36] M.A. Islam, A. Karim, C.W. Woon, B. Ethiraj, C.K. Cheng, A. Yousuf, M.M.R. Khan, Augmentation of air cathode microbial fuel cell performance using wild type *Klebsiella variicola*, RSC Advances 7(8) (2017) 4798-4805.

[37] O. Tkach, L. Liu, A. Wang, Electricity Generation by Enterobacter sp. of Single-Chamber Microbial Fuel Cells at Different Temperatures, Journal of Clean Energy Technologies 4(1) (2015) 36.

[38] F. Vicari, S. Mateo, F. Fernandez-Morales, P. Cañizares, A. Galia, O. Scialdone, M. Rodrigo, Influence of the methodology of inoculation in the performance of air-breathing microbial fuel cells, J. Electroanal. Chem. 803 (2017) 81-88.

[39] F. Vicari, A. D'Angelo, A. Galia, P. Quatrini, O. Scialdone, A single-chamber membraneless microbial fuel cell exposed to air using *Shewanella putrefaciens*, J. Electroanal. Chem. 783 (2016) 268-273.

[40] H. Leclerc, L. Schwartzbrod, E. Dei-Cas, Microbial agents associated with waterborne diseases, Crit. Rev. Microbiol. 28(4) (2002) 371-409.

[41] A. Rochex, J.-M. Lebeault, Effects of nutrients on biofilm formation and detachment of a *Pseudomonas putida* strain isolated from a paper machine, Water Res. 41(13) (2007) 2885-2892.

[42] C.M. Manuel, O.C. Nunes, L. Melo, Dynamics of drinking water biofilm in flow/non-flow conditions, Water Res. 41(3) (2007) 551-562.

[43] Y. Abe, S. Skali-Lami, J.-C. Block, G. Francius, Cohesiveness and hydrodynamic properties of young drinking water biofilms, Water Res. 46(4) (2012) 1155-1166.

[44] E. Paul, J.C. Ochoa, Y. Pechaud, Y. Liu, A. Liné, Effect of shear stress and growth conditions on detachment and physical properties of biofilms, Water Res. 46(17) (2012) 5499-5508.

Figure captions

Fig. 1 Performance trend of MFC_1, a) profile of power densities vs COD removal with time, b) polarization curves of MFC on different days of MFC operations, c) cyclic voltammograms on different days of MFC operations, d) fitting results of Nyquist plots on different days of MFC operation, e) the biofilm visualization on the 3rd day, f) the biofilm visualization on the 11th day, g) the biofilm visualization on the 21st day, h) the cell viability count of anode biofilm on different days of operation

Fig. 2 Performance of MFC_2, a) current generation trend under fixed external resistance of 1000 Ω. b) FESEM images on carbon felt on the 21st day, c) FESEM images on carbon felt on the 22nd day, d) cell viability count of biofilm on different days of operations, e) Nyquist plots on different days of operations, f) cyclic voltammograms on different days of operations

Fig. 3 Effect of different shear stresses on MFC performance, a) the current generation trend (under fixed external resistance of 1000 Ω) for the shear stress of 4.38 mPa, b) the current generation trend (under fixed external resistance of 1000 Ω) for the shear stress of 9.34 mPa, c) the current generation trend (under fixed external resistance of 1000 Ω) for the shear stress of

14.32 mPa, and d) polarization curve of MFCs under different shear stresses on the 25th day of operation

Fig. 4 Visualization of biofilm at different shear stresses, a) virgin, b) low shear stress of 4.38 mPa, c) moderate shear stress of 9.34 mPa and d) high shear stress of 14.92 mPa

Fig. 5 Electrochemical characterization of MFCs using different shear stresses, a) Cyclic voltammograms for different shear stress and b) Nyquist plots on 25th day for different shear stresses

Highlights

- Accumulation of dead cells in the biofilm reduced the power generation in MFCs
- Polarization resistance increased due to the formation of ineffective biofilm
- Moderate shear stress successfully revitalized biofilm and restored power in MFC

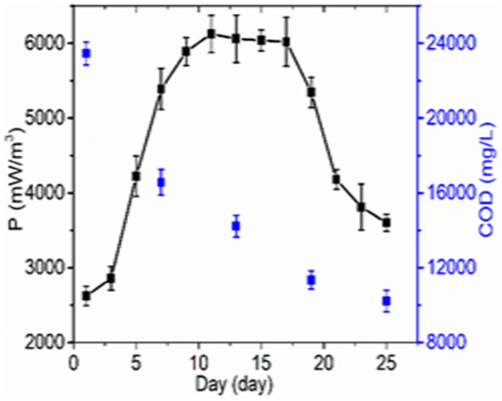

a

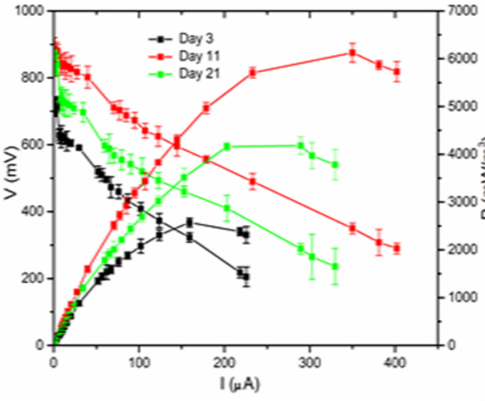

b

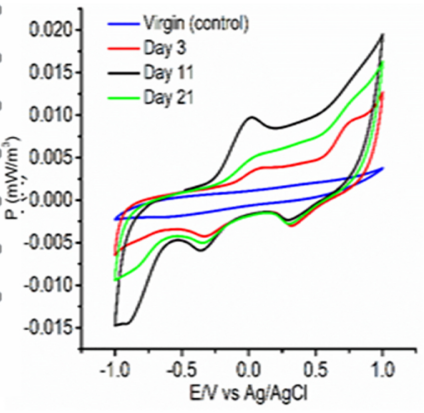

c

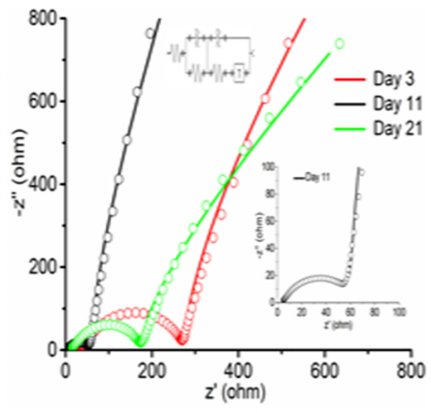

d

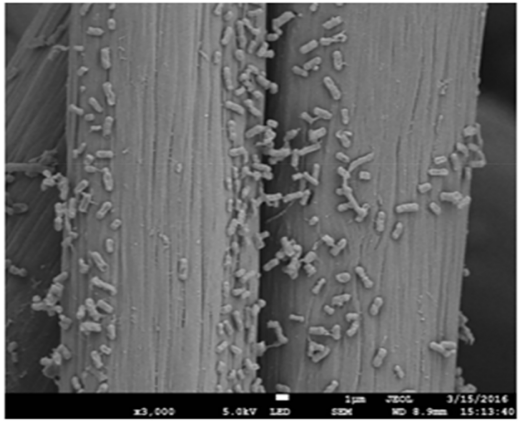

e

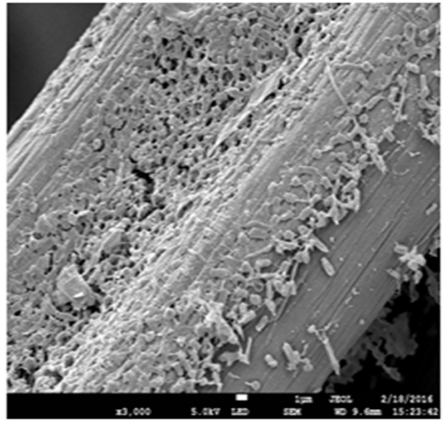

f

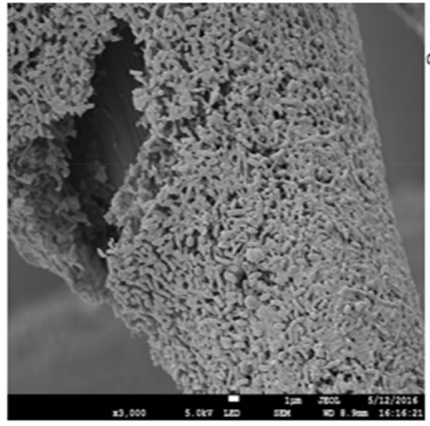

g

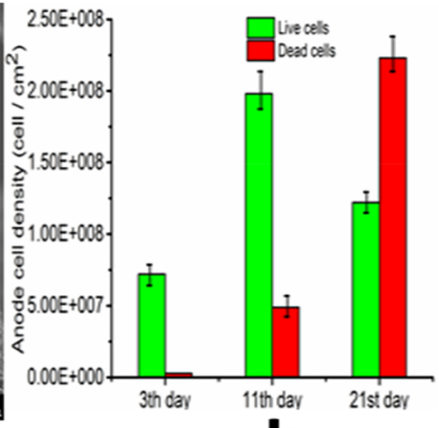

h

Figure 1

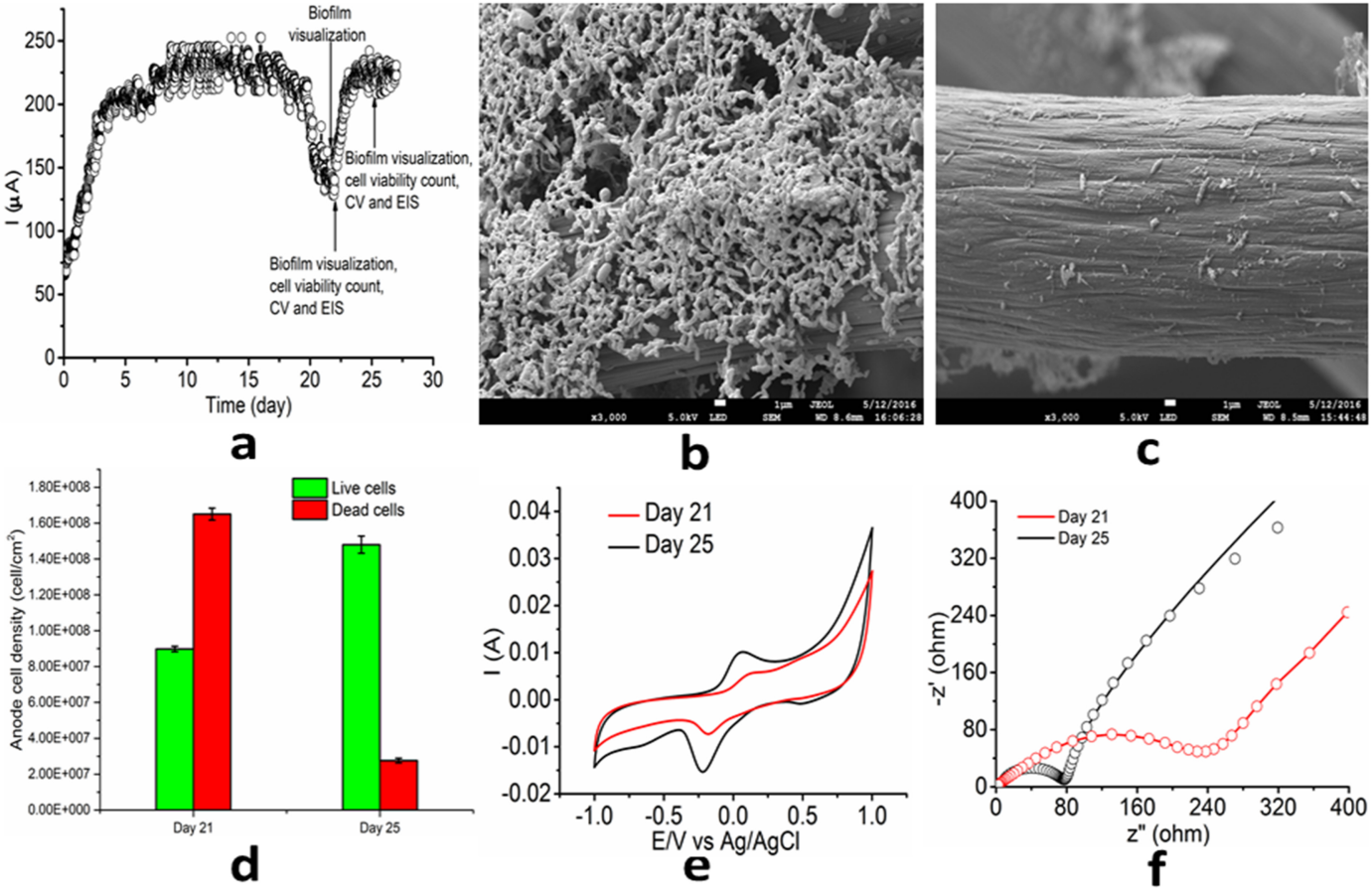
Biofilm visualization
Biofilm visualization, cell viability count, CV and EIS
Biofilm visualization, cell viability count, CV and EIS
I (μA)
Time (day)
a
b
c
Live cells
Dead cells
Anode cell density (cell/cm²)
Day 21
Day 25
d
Day 21
Day 25
I (A)
E/V vs Ag/AgCl
e
Day 21
Day 25
-z' (ohm)
z" (ohm)
f

Figure 2

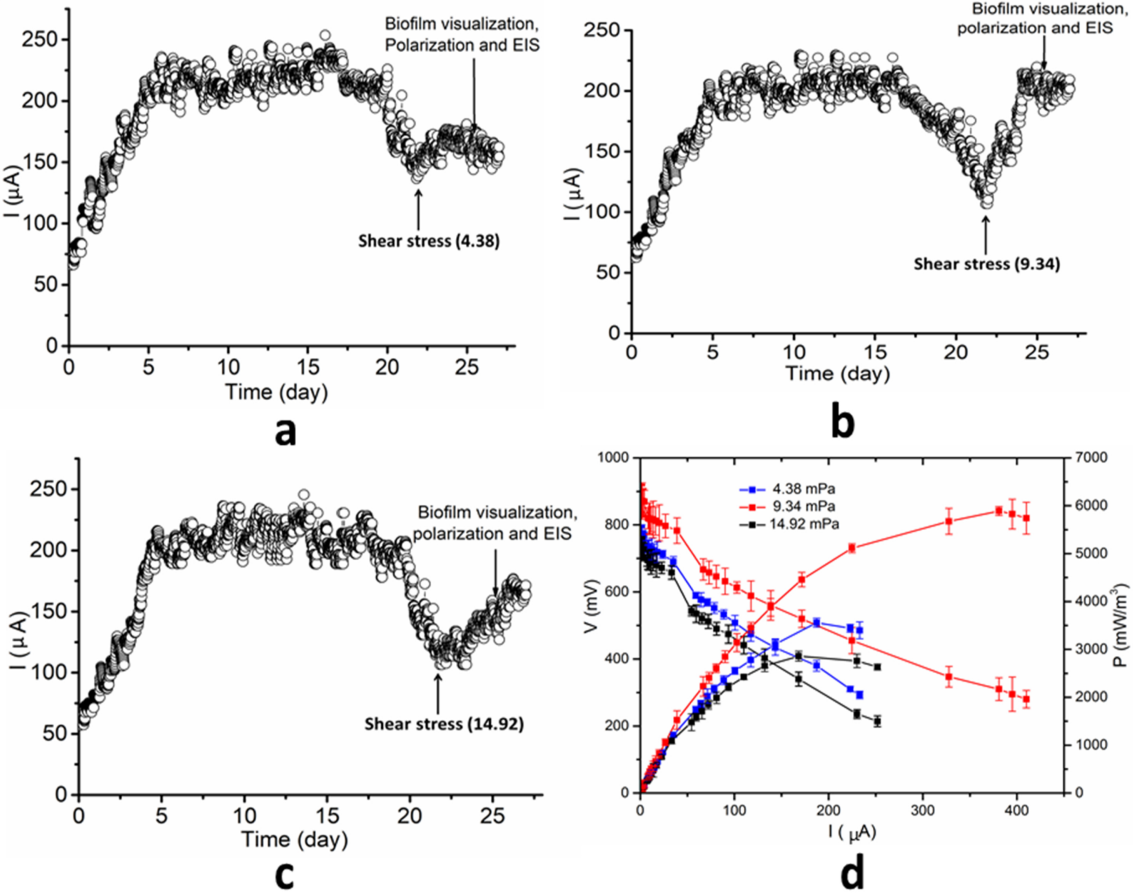
Biofilm visualization, Polarization and EIS
Shear stress (4.38)
I (μA)
Time (day)
a
Biofilm visualization, polarization and EIS
Shear stress (9.34)
I (μA)
Time (day)
b
Biofilm visualization, polarization and EIS
Shear stress (14.92)
I (μA)
Time (day)
c
4.38 mPa
9.34 mPa
14.92 mPa
V (mV)
P (mW/m3)
I (μA)
d

Figure 3

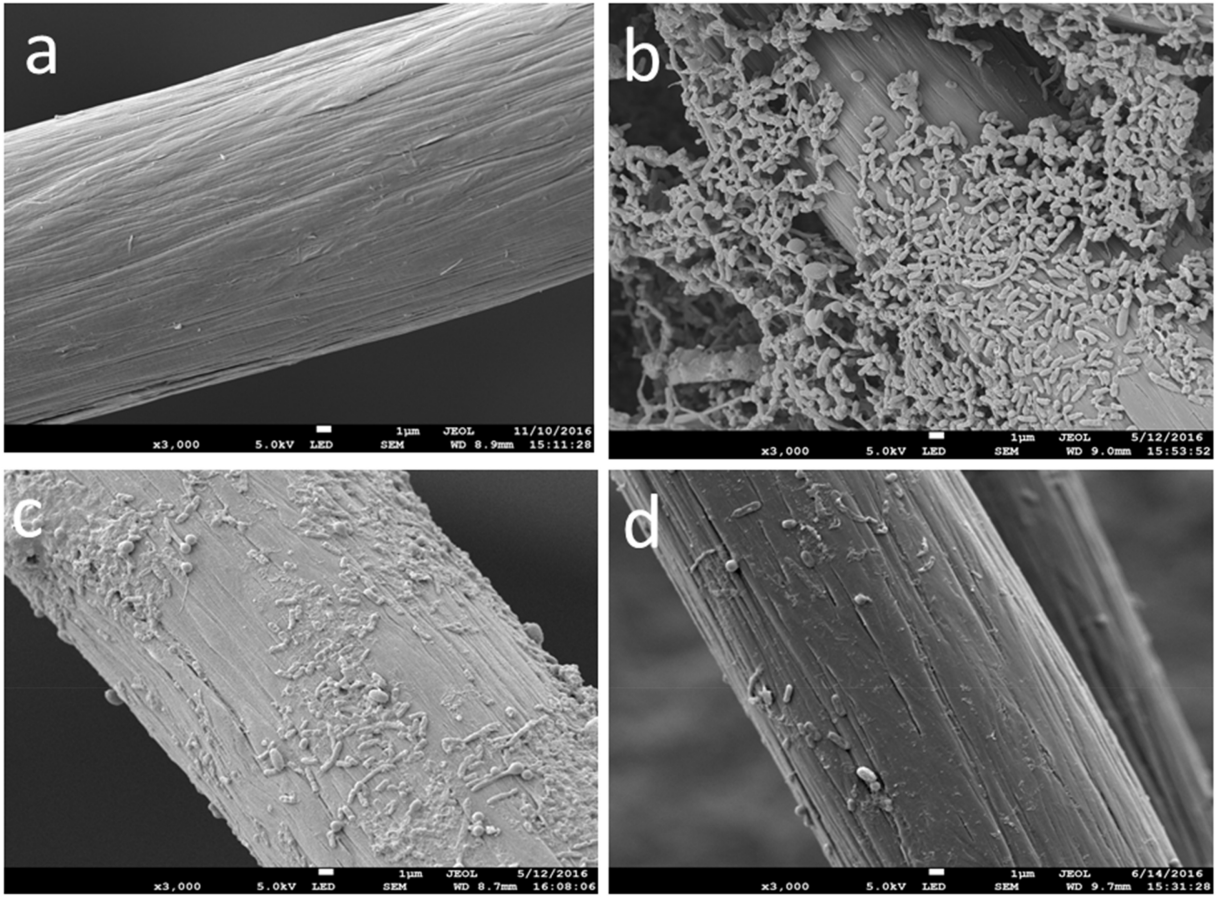
a
x3,000 5.0kV LED 1µm JEOL SEM 11/10/2016 WD 8.9mm 15:11:28
b
x3,000 5.0kV LED 1µm JEOL SEM 5/12/2016 WD 9.0mm 15:53:52
c
x3,000 5.0kV LED 1µm JEOL SEM 5/12/2016 WD 8.7mm 16:08:06
d
x3,000 5.0kV LED 1µm JEOL SEM 6/14/2016 WD 9.7mm 15:31:28

Figure 4

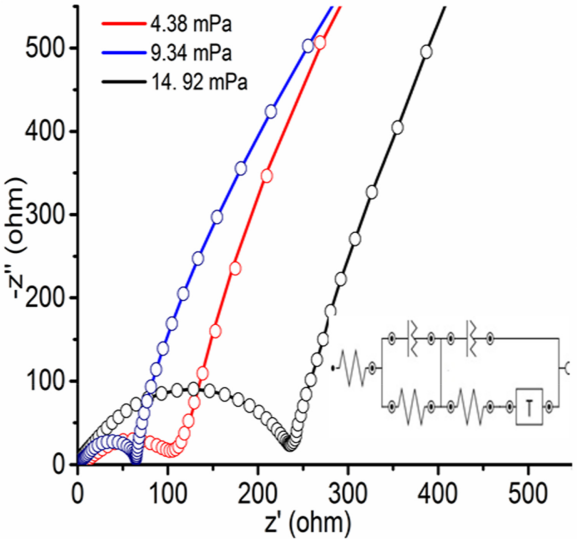
4.38 mPa
9.34 mPa
14. 92 mPa
-z'' (ohm)
z' (ohm)
0
100
200
300
400
500
T

a

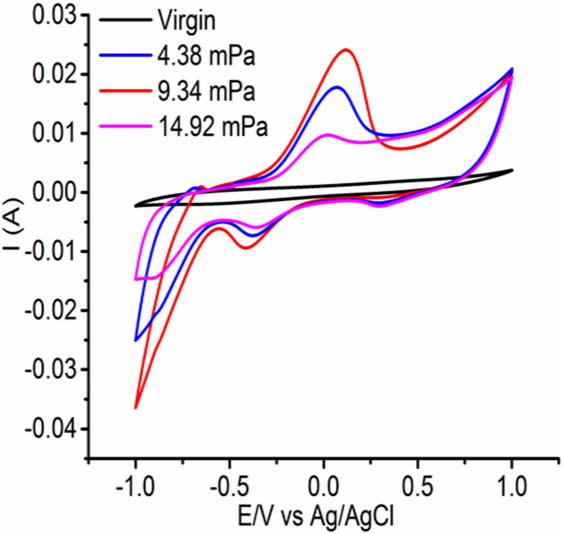
Virgin
4.38 mPa
9.34 mPa
14.92 mPa
I (A)
E/V vs Ag/AgCl
0.03
0.02
0.01
0.00
-0.01
-0.02
-0.03
-0.04
-1.0
-0.5
0.0
0.5
1.0

b

Figure 5